Transfer Matrix Approach to Classical Systems

T. Nishino 1, K. Okunishi 2, Y. Hieida 2, T. Hikihara 1, and H. Takasaki 1

[1] Department of Physics, Graduate School of Science and Technology, Kobe University, Rokko-dai, Nada, Kobe 657-8501, Japan
[2] Department of Physics, Graduate School of Science, Osaka University, Toyonaka, Osaka 560-0043, Japan

Establishment of the DMRG by White is one of the major progress in computational condensed matter physics. [1] DMRG enables us to calculate ground states of relatively large scale one-dimensional (1D) quantum systems. Since 1D quantum systems are deeply related to 2D classical systems, [2–4] it is natural to try to apply DMRG to 2D classical systems. The infinite system algorithm was first applied to the Ising model. [5] After that, Carlon *et al* applied the finite system algorithm to the Potts models. [6–8] They obtained very accurate density profiles and critical indices. Later, the DMRG formulation for classical systems is applied to 1D quantum system at finite temperature. [9–11]

In this article we explain the variational background of DMRG applied to 2D classical models, where the trial state is written in a product of matrices. It is worth knowing that such a matrix-product Ansatz originates with Kramers and Wannier, [12,13] though DMRG was established totally independent from their *classical work*. As a prelude to DMRG, first let us glance at the brief history of the matrix-product Ansatzs.

1 Introduction to Matrix Product Ansatzs

Consider a variational problem for a row-to-row transfer matrix T of a 2D classical lattice model. The variational partition function per row is written as

$$\lambda = \frac{\boldsymbol{u}^T\, T\, \boldsymbol{v}}{\boldsymbol{u}^T\, \boldsymbol{v}} = \frac{\langle u|T|v\rangle}{\langle u|v\rangle}\,, \tag{1}$$

where $\boldsymbol{u}$ and $\boldsymbol{v}$ are variational states. The Rayleigh ratio λ is maximized when $\boldsymbol{u}$ and $\boldsymbol{v}$ coincide with the left and the right eigenvectors of T, respectively. (Note that $\boldsymbol{u} \neq \boldsymbol{v}$ when T is asymmetric. [14]) If one wishes to apply the variational formula for a practical problem, $\boldsymbol{u}$ and $\boldsymbol{v}$ should satisfy the following requirements

- The calculation of λ for a given pair of $\boldsymbol{u}$ and $\boldsymbol{v}$ is very easy.
- The variational state has locality in some sense, that enables its local refinement. (A global change is much more time consuming.)

In 1941 Klamers and Wannier (K-W) [12] investigated such a variational problem for the square lattice Ising model, assuming that the variatonal state $v(\ldots, s_{i-1}, s_i, s_{i+1}, s_{i+2}, \ldots)$ can be written as a matrix product

$$\ldots F(s_{i-1}|s_i)F(s_i|s_{i+1})F(s_{i+1}|s_{i+2})\ldots , \tag{2}$$

where $s_i = \pm 1$ is the Ising variables at i-site, and $F(s|s')$ is a 2-dimensional symmetric matrix. We use the notation "(|)" when we explicitly show the matrix indices; for example, $A_{ij} = A(i|j)$. The calculated transition temperature T_c and the specific heat are more accurate than those obtained by the molecular-field and the Bethe approximations. [15] It should be noted that the Gutzwiller approximation [16] for the Hubbard Model [17,18] is quite close to the K-W approximation.

Around 1960-70 Baxter improved the K-W approximation by introducing additional freedom. [19,20] His variational state $v(\ldots, s_{i-1}, s_i, s_{i+1}, s_{i+2}, \ldots)$ is written as

$$\sum_{\ldots,a,b,c,d,\ldots} \ldots F_{ab}(s_{i-1}|s_i)F_{bc}(s_i|s_{i+1})F_{cd}(s_{i+1}|s_{i+2})\ldots , \tag{3}$$

where $\ldots a$, b, c, $d \ldots$, denote the additional m-state variables. Since $F_{ab}(s|s')$ contains $4m^2$ adjustable parameters, the way of finding out the best $F_{ab}(s|s')$ that maximizes λ (Eq.1) is non trivial. He performed the maximization using a self-consistent equation about the corner transfer matrix. (CTM) [20]

Applications of the matrix product formulation to quantum systems began with the investigations of Haldane's conjecture. In 1985 Nightingale and Blöte [21] used the K-W matrix product (Eq.2) as the initial vector of their projector Monte Carlo simulation. It is interesting that they commented about Baxter's method as "... *This method was formulated by Baxter for classical models in statistical mechanics. The generalization to quantum mechanical system is straightforward.*" In 1987 Affleck, Lieb, Kennedy, and Tasaki [22] showed that the ground-state $\psi(\ldots, s_{i-1}, s_i, s_{i+1}, s_{i+2}, \ldots)$ of a special $S = 1$ spin chain can be exactly expressed as

$$\sum_{\ldots,a,b,c,d,e,\ldots} \ldots M_{ab}(s_{i-1})M_{bc}(s_i)M_{cd}(s_{i+1})M_{de}(s_{i+2})\ldots , \tag{4}$$

where $\ldots, a, b, c, d, e, \ldots$ are 2-state variables. Fannes et. al. generalized the above wave function by assigning m-degree of freedom to $\ldots, a, b, c, d, e, \ldots$. Their variational state is known as 'finitely correlated state', since the correlation length is always finite. [23,24] Although ψ in Eq.4 does not look like $\boldsymbol{v}$ in Eq.3, they are essentially the same; they are related by a duality transformation. Such a variational state written in matrix product has been developed independently in the field of exclusion process. [25–28]

Since the matrices are position independent in Eqs.2-4, it is impossible to apply these variational methods to any system that does not have the

translational invariance. The variational state $\phi(\ldots, s_{i-1}, s_i, s_{i+1}, s_{i+2}, \ldots)$ in DMRG

$$\sum_{\ldots,a,b,c,d,e,\ldots} \ldots M_{ab}(s_{i-1}) M'_{bc}(s_i) M''_{cd}(s_{i+1}) M'''_{de}(s_{i+2}) \ldots \tag{5}$$

is more flexible, where not only the matrix elements, but also the matrix size can be position dependent. Compare to Eqs.2-4, the following points are improved.

- The position dependence of the matrix enables us to treat a system that does not have translational invariance.
- Local improvements for ϕ is possible via modifications of local matrices. [29]

The construction of variational state has been an important subject for analytical investigation of DMRG. [30,31]

We explain the way to apply DMRG to 2D classical models, chiefly by considering the variational state written in the matrix product. The order of subjects in the following sections are reversal the conventional one, since we start from the variational background in DMRG. [32] In the next section we introduce the square lattice Ising model as an example of 2D classical models. The density matrix is introduced in §3 as a preparation for the block spin transformation. In §4 we decompose the eigenvector of the transfer matrix into the product of local matrices. An example of variational state is presented in §5 through a freedom restriction for the matrix product. In §6 we introduce the standard form for the variational state that is used in the numerical calculation of the finite system algorithm. We explain the numerical detail in §7 (finite system algorithm) and in §8 (infinite system algorithm). We finally discuss the corner transfer matrix formulation and its generalization to 3D in the last section.

2 Transfer Matrix

As an example of 2D systems, let us consider the square lattice Ising model [35] on a cylinder, which is defined by imposing periodic boundary condition in the vertical direction of N (= horizontal width) by ℓ (= vertical length) spin lattice. We consider the open boundary condition for the horizontal direction. The system consists of ℓ numbers of rows of width N. Since we always consider the limit $\ell \to \infty$, we refer N as the system size. We label the spins in a row from the left to right $s_1, s_2, \ldots, s_{N-1}, s_N$, where we normally write it using the notation $s_{1\ldots}s_N$ for book keeping. Following the convention in DMRG, we divide the spin row into the left $s_{1\ldots}s_M$ and the right $s_{M+1\ldots}s_N$. Since the width of the row $s_{1\ldots}s_N$ is always fixed to N, we often abbreviate $s_{1\ldots}s_M$ as $\ldots s_M$, and $s_{M+1\ldots}s_N$ as $s_{M+1\ldots}$, by dropping the symbols "s_1" and "s_N".

When the Ising interaction Js_is_j is restricted to the nearest neighbor, the transfer matrix is written as a 2^N-dimensional matrix

$$T(s'_{1\ldots}s'_N|s_{1\ldots}s_N) \;=\; \exp\left\{\frac{K}{2}\sum_{i=1}^{N-1}(s'_is'_{i+1}+s_is_{i+1})+K\sum_{i=1}^{N}s'_is_i\right\}, \quad (6)$$

where K is the parameter $-J/k_{\rm B}T$. We consider the open boundary condition in the following. [33] As we have divided the spin row into $s_{1\ldots}s_M$ and $s_{M+1\ldots}s_N$, we divide the transfer matrix T into the left and the right

$$T_L(s'_{1\ldots}s'_M|s_{1\ldots}s_M) \;=\; \exp\left(\frac{K}{2}\,s'_1s_1\right)\prod_{i=1}^{M-1}W(s'_is'_{i+1}|s_is_{i+1})$$

$$T_R(s'_{M+1\ldots}s'_N|s_{M+1\ldots}s_N) \;=\; \exp\left(\frac{K}{2}s'_Ns_N\right)\prod_{i=M+1}^{N-1}W(s'_is'_{i+1}|s_is_{i+1}), \quad (7)$$

where $W(s'_is'_{i+1}|s_is_{i+1})$ is the local Boltzmann weight defined as

$$\exp\left\{\frac{K}{2}\left(s_is_{i+1}+s_{i+1}s'_{i+1}+s'_{i+1}s'_i+s'_is_i\right)\right\}. \quad (8)$$

From the matrices T_L, W and T_R, the transfer matrix is reconstructed as

$$\begin{aligned}&T(s'_{1\ldots}s'_N|s_{1\ldots}s_N)\\ &= \quad T_L(_{\ldots}s'_M|_{\ldots}s_M)W(s'_Ms'_{M+1}|s_Ms_{M+1})T_R(s'_{M+1\ldots}|s_{M+1\ldots}).\end{aligned} \quad (9)$$

Generally speaking, the transfer matrix is not always symmetric. [14] For example, if there is interaction in the diagonal direction of the square lattice, the Boltzmann weight is modified as

$$W_d(s'_is'_{i+1}|s_is_{i+1}) = W(s'_is'_{i+1}|s_is_{i+1})\exp\left\{K's_is'_{i+1}+K''s'_is_{i+1}\right\}, \quad (10)$$

and the transfer matrix T is asymmetric when $K'\neq K''$. More generally, it is possible to treat various models such as

- The q-state Potts model [34] or the n-vector model, that have *discrete spin symmetry and short range interaction.*
- The interaction round a face (IRF) model [20] whose Boltzmann weight $W(s'_is'_{i+1}|s_is_{i+1})$ is expressed by *arbitrary square matrix.*

in the framework of DMRG. For a tutorial purpose, we only consider the symmetric transfer matrix of the Ising model in the following.

3 Eigenvalues of the Density Submatrix

The density matrix of the N by ℓ cylindrical system is simply the ℓ-th power of the transfer matrix: $\rho = T^{\,\ell}$. The partition function is its trace

$$Z \;=\; {\rm Tr}\,\rho \;=\; {\rm Tr}\left\{T^\ell\right\} \;=\; \sum_{\kappa=1}^{2^N}\lambda_\kappa^{\,\ell}, \quad (11)$$

where λ_κ is the eigenvalue of T in the decreasing order $\lambda_1 \geq \lambda_2 \geq \cdots \lambda_{2^N} \geq 0$. When ℓ is sufficiently large, the partition function Z can be expressed as $Z \simeq {\lambda_1}^\ell$, where the symbol "$\simeq$" denotes that the ratio ${\lambda_1}^\ell / Z$ converges to unity for $\ell \to \infty$. Under this situation, the density matrix can be written as

$$\rho \simeq \boldsymbol{v}\, {\lambda_1}^\ell\, \boldsymbol{v}^T = |v\rangle\, {\lambda_1}^\ell\, \langle v| \tag{12}$$

where $\boldsymbol{v}$ is the eigenvector of T that corresponds to λ_1. We assume the normalization $\langle v|v\rangle = \boldsymbol{v}^T\, \boldsymbol{v} = 1$. Here after we consider the density matrix constructed by Eq.12.

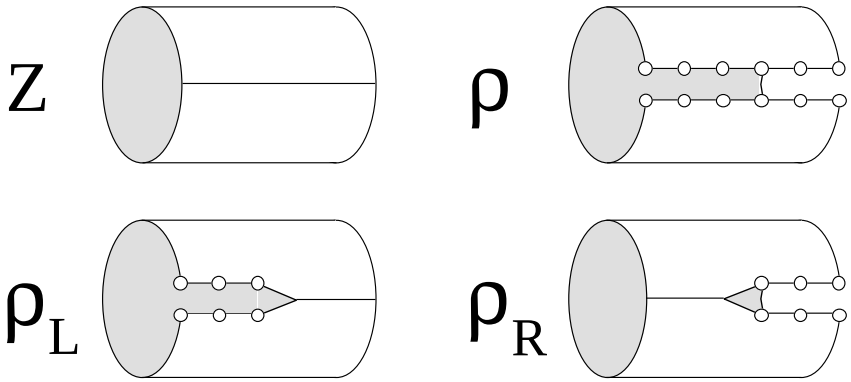

Fig. 1. Graphical representation for Z (Eq.11), ρ (Eq.12), ρ_L and ρ_R (Eq.13). The DSM can be interpreted as a 'cut' on 2D system.

What they call 'density matrix' in the context of DMRG is not the density matrix itself, but is the density submatrix, (DSM) which is obtained by partially tracing out spin variables from ρ. The DSM for the left and the right sides are defined as [36]

$$\begin{aligned} \rho_L(\ldots s'_M|\ldots s_M) &= \sum_{s_{M+1}\cdots s_N} \rho(\ldots s'_M\, s_{M+1}\ldots s_N|\ldots s_M\, s_{M+1}\ldots s_N) \\ \rho_R(s'_{M+1}\ldots|s_{M+1}\ldots) &= \sum_{s_1\cdots s_M} \rho(s_1\ldots s_M\, s'_{M+1}\ldots|s_1\ldots s_M\, s_{M+1}\ldots)\,. \end{aligned} \tag{13}$$

Figure 1 shows the graphical representation of the density submatrix; ρ_L and ρ_R correspond to cuts on the cylinder. [32] To take the trace of DSM is to join the cut to reconstruct the cylinder, and therefore $Z = \mathrm{Tr}\,\rho_L = \mathrm{Tr}\,\rho_R$.

Using Eq.12, we can also construct DSM in this way

$$\rho_L(\ldots s'_M|\ldots s_M) \simeq \sum_{s_{M+1}\cdots s_N} v(\ldots s'_M\, s_{M+1}\ldots s_N)\, {\lambda_1}^{\ell}\, v(\ldots s_M\, s_{M+1}\ldots s_N)$$
$$\rho_R(s'_{M+1}\ldots|s_{M+1}\ldots) \simeq \sum_{s_1\cdots s_M} v(s_1\ldots s_M\, s'_{M+1}\ldots)\, {\lambda_1}^{\ell}\, v(s_1\ldots s_M\, s_{M+1}\ldots)\,, \quad (14)$$

when ℓ is sufficiently large. The rank of both ρ_L and ρ_R thus created is equal to $r = \min(2^M, 2^{N-M}) = 2^{\min(M,N-M)}$.

Diagonalizations of the density submatrices are one of the important processes in DMRG; ρ_L and ρ_R can be expressed as

$$\rho_L = \sum_{\xi=1}^{2^M} \boldsymbol{a}_\xi\, {\omega_\xi}^2\, {\boldsymbol{a}_\xi}^T \qquad \rho_R = \sum_{\zeta=1}^{2^{N-M}} \boldsymbol{b}_\zeta\, {\mu_\zeta}^2\, {\boldsymbol{b}_\zeta}^T\,, \quad (15)$$

where $\boldsymbol{a}_\xi$ and $\boldsymbol{b}_\xi$ are eigenvectors of ρ_L and ρ_R, respectively. The eigenvectors satisfy the orthogonal relations ${\boldsymbol{a}_\xi}^T \boldsymbol{a}_{\xi'} = \delta_{\xi\xi'}$ and ${\boldsymbol{b}_\zeta}^T \boldsymbol{b}_{\zeta'} = \delta_{\zeta\zeta'}$, and they are complete

$$I_L = \sum_{\xi=1}^{2^M} \boldsymbol{a}_\xi\, {\boldsymbol{a}_\xi}^T \qquad I_R = \sum_{\zeta=1}^{2^{N-M}} \boldsymbol{b}_\zeta\, {\boldsymbol{b}_\zeta}^T\,, \quad (16)$$

where I_L and I_R are 2^M- and 2^{N-M}-dimensional unit matrices, respectively. It is convenient to define orthogonal matrices $A = (\boldsymbol{a}_1, \boldsymbol{a}_2, \cdots, \boldsymbol{a}_{2^M})$ and $B = (\boldsymbol{b}_1, \boldsymbol{b}_2, \cdots, \boldsymbol{b}_{2^{N-M}})$. We use them when we explicitly show the spin indices. For example, Eq.15 can be written as

$$\rho_L(\ldots s'_M|\ldots s_M) = \sum_{\xi=1}^{2^M} A(s'_1\ldots s'_M|\xi)\, {\omega_\xi}^2\, A(s_1\ldots s_M|\xi)$$
$$\rho_R(s'_{M+1}\ldots|s_{M+1}\ldots) = \sum_{\zeta=1}^{2^{N-M}} B(s'_{M+1}\ldots s'_N|\zeta)\, {\mu_\zeta}^2\, B(s_{M+1}\ldots s_N|\zeta)\,. \quad (17)$$

In Eqs.15 and 17 we have expressed the eigenvalues of ρ_L and ρ_R as squares of real numbers, because normally they are non-negative. [37] As for the eigenvalues of ρ, we assume the decreasing order for both ${\omega_\xi}^2$ and ${\mu_\zeta}^2$

$${\omega_1}^2 \geq {\omega_2}^2 \geq \cdots \omega^2_{2^M} \geq 0 \qquad {\mu_1}^2 \geq {\mu_2}^2 \geq \cdots \mu^2_{2^{N-M}} \geq 0\,. \quad (18)$$

Actually, ${\omega_i}^2 = {\mu_i}^2$ holds for $i \leq r = \min(2^M, 2^{N-M})$, and the rest ($i > r$) are zero. The partition function is therefore equal to

$$Z \simeq {\omega_1}^2 + {\omega_2}^2 + \cdots + {\omega_r}^2 = {\mu_1}^2 + {\mu_2}^2 + \cdots + {\mu_r}^2\,. \quad (19)$$

Unlike the density matrix ρ, not only the largest eigenvalue is dominant for DSM. This is because the spin rows $s'_{1\cdots}s'_M$ and $s_{1\cdots}s_M$ in $\rho_L(\cdots s'_M|\cdots s_M)$ are correlated to through the junction $s_{M+1\cdots}s_N$. (Eq.13) Roughly speaking, the number of dominant eigenvalues of DSM is an increasing function of the correlation length of the system.

The diagonalizations of DSM (Eq.17) suggests that the eigenvector of the transfer matrix can be decomposed as

$$v(s_{1\cdots}s_N) \;=\; \sum_{\xi=1}^{r} A(s_{1\cdots}s_M|\xi)\;\frac{\omega_\xi}{\sqrt{Z}}\;B(s_{M+1\cdots}s_N|\xi)\,. \tag{20}$$

One can check that Eq.20 draws Eq.17 with the help of $A^{-1} = A^T$ and $B^{-1} = B^T$. Such a decomposition is known as the singular value decomposition, [38] (SVD) where $\omega_\xi/\sqrt{Z}$ is called as the *singular value*. We can further decompose A and B into local factors, as we show in the next section.

4 Matrix Product Decomposition

The matrix $A(s_{1\cdots}s_M|\xi)$ represents an *exact* block-spin transformation from $s_{1\cdots}s_M$ to 2^M-state variable ξ; we write ξ as ξ_M in the following. We also write ζ of $B(s_{M+1\cdots}|\zeta)$ as ζ_{M+1} in the same way. Let us apply the transformation $s_{1\cdots}s_{M-1} \to \xi_{M-1}$ to $\rho_L(s'_{1\cdots}s'_{M-1}s'_M|s_{1\cdots}s_{M-1}s_M)$ by applying A

$$\sum_{\substack{s'_1\cdots s'_{M-1}\\ s_1\cdots s_{M-1}}} A(\cdots s'_{M-1}|\xi'_{M-1})\rho_L(\cdots s'_{M-1}s'_M|\cdots s_{M-1}s_M)A(\cdots s_{M-1}|\xi_{M-1}) \tag{21}$$

to obtain $\rho_L(\xi'_{M-1}s'_M|\xi_{M-1}s_M)$. The matrix $\rho_L(\xi'_{M-1}s'_M|\xi_{M-1}s_M)$ can be interpreted a DSM for the spin pair $\xi_{M-1}s_M$. We then obtain a new matrix $A(\xi_{M-1}s_M|\xi_M)$ through the diagonalization of the transformed DSM

$$\rho_L(\xi'_{M-1}s'_M|\xi_{M-1}s_M) = \sum_{\xi_M=1}^{r} A(\xi'_{M-1}s'_M|\xi_M)\;\omega_{\xi_M}^2\;A(\xi_{M-1}s_M|\xi_M)\,. \tag{22}$$

From Eqs.21-22, it is apparent that $A(\xi_{M-1}s_M|\xi_M)$ is defined as (Fig.2)

$$A(\xi_{M-1}s_M|\xi_M) = \sum_{s_1\cdots s_{M-1}} A(s_{1\cdots}s_{M-1}|\xi_{M-1})\,A(s_{1\cdots}s_{M-1}s_M|\xi_M)\,. \tag{23}$$

In the same way, we obtain $B(s_{M+1}\zeta_{M+2}|\zeta_{M+1})$ as

$$\sum_{s_{M+2}\cdots s_N} B(s_{M+2\cdots}s_N|\zeta_{M+2})\,B(s_{M+1}s_{M+2\cdots}s_N|\zeta_{M+1}) \tag{24}$$

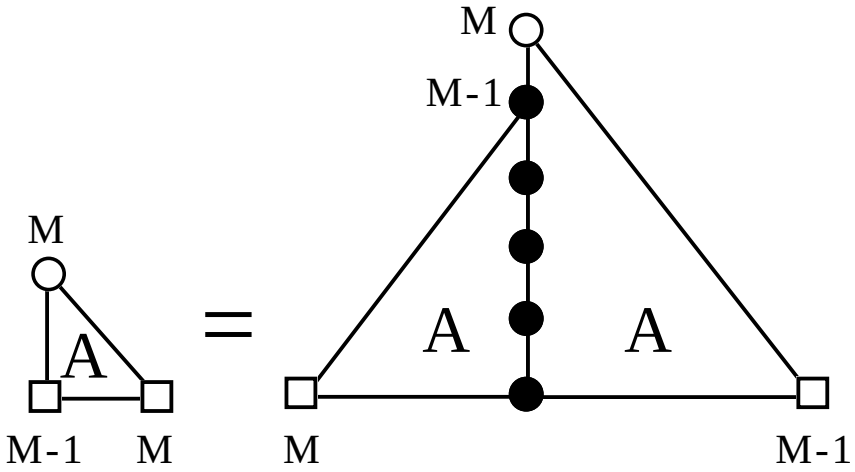

Fig. 2. Definition of $A(\xi_{M-1}s_M|\xi_M)$ in Eq.23. Circles and squares are the Ising spins and the block spins, respectively.

by considering $\rho_R(s'_{M+1}\zeta'_{M+2}|s_{M+1}\zeta_{M+2})$, which is defined as

$$\sum_{s'_{M+2\cdots}s'_N, s_{M+2\cdots}s_N} B(s'_{M+2\cdots}|\zeta'_{M+2})\ \ \rho_R(s'_{M+1}s'_{M+2\cdots}|s_{M+1}s_{M+2\cdots}) \\ B(s_{M+2\cdots}|\zeta_{M+2})\,. \qquad (25)$$

At this point, we find a recursion relation from the definition of the identity matrix I_L (Eq.16)

$$\begin{aligned} A(\ldots s_M|\xi_M) &= \sum_{s'_1\cdots s'_{M-1}} I(\ldots s_{M-1}|\ldots s'_{M-1})A(\ldots s'_{M-1}s_M|\xi_M) \\ &= \sum_{\xi_{M-1}\ s'_1\cdots s'_{M-1}} A(\ldots s_{M-1}|\xi_{M-1})A(\ldots s'_{M-1}|\xi_{M-1})A(\ldots s'_{M-1}s_M|\xi_M) \\ &= \sum_{\xi_{M-1}} A(\ldots s_{M-1}|\xi_{M-1})A(\xi_{M-1}s_M|\xi_M)\,, \qquad (26) \end{aligned}$$

which enables the successive decomposition

$$\begin{aligned} &= \sum_{\xi_{M-2}\xi_{M-1}} A(\ldots s_{M-2}|\xi_{M-2})A(\xi_{M-2}s_{M-1}|\xi_{M-1})A(\xi_{M-1}s_M|\xi_M) \\ &= \sum_{\xi_2\cdots\xi_{M-1}} A(s_1s_2|\xi_2)A(\xi_2s_3|\xi_3)\cdots A(\xi_{M-1}s_M|\xi_M)\,. \qquad (27) \end{aligned}$$

In the same way, we can decompose B into the matrix product form

$$B(s_{M+1\cdots}|\zeta_{M+1}) \;=\; \sum_{\zeta_{M+2}\cdots\zeta_{N-1}} \prod_{j=M+1}^{N-1} B(s_j\zeta_{j+1}|\zeta_j)\,, \tag{28}$$

where we have written s_N as ζ_N.

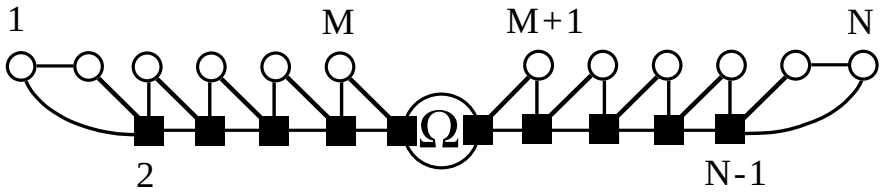

Fig. 3. Matrix product decomposition of the state vector. (Eq.29)

Substituting these matrix product decompositions into Eq.20, we obtain the complete decomposition of the eigenvector $v(s_{1\cdots}s_N)$ into the form (Fig.3)

$$\sum_{\{\xi\}\{\zeta\}} \prod_{i=2}^{M} A(\xi_{i-1}s_i|\xi_i)\; \Omega(\xi_M|\zeta_{M+1}) \prod_{j=M+1}^{N-1} B(s_j\zeta_{j+1}|\zeta_j)\,, \tag{29}$$

where sum is taken over for ξ_2, $\cdots$ ξ_M and ζ_{M+1}, $\cdots$ ζ_{N-1} that are shown by black squares in Fig.3. The new matrix $\Omega(\xi_M|\zeta_{M+1})$ is a r-dimensional diagonal matrix: $\Omega(\xi_M|\zeta_{M+1}) \;=\; \delta_{\xi_M\zeta_{M+1}}\omega_{\xi_M}/\sqrt{Z}$. (Strictly speaking, Ω need not to be diagonal, if it satisfies $\Omega\Omega^T = 1$.) The trace of Ω^2 is equal to unity. The decomposition is formally dependent on the initial division of the system. If we divide the spin row $s_{1\cdots}s_N$ at the point $M+1$, we obtain a decomposition in another form

$$\sum_{\{\xi\}\{\zeta\}} \prod_{i=2}^{M+1} A(\xi_{i-1}s_i|\xi_i)\,\Omega(\xi_{M+1}|\zeta_{M+2}) \prod_{j=M+2}^{N-1} B(s_j\zeta_{j+1}|\zeta_j)\,. \tag{30}$$

Since Eq.30 is the same as Eq.29, there should be a relation [39]

$$\Omega(\xi_M|\zeta_{M+1})B(s_{M+1}\zeta_{M+2}|\zeta_{M+1}) = A(\xi_M s_{M+1}|\xi_{M+1})\Omega(\xi_{M+1}|\zeta_{M+2})\,. \tag{31}$$

5 Restriction for the Matrix Product

So far as we try to *exactly* express the eigenvectors of T by the matrix product, we have to treat large dimensional matrices. For example, the matrix dimension of $A(\xi_{M-1}s_M|\xi_M)$ is 2^M, which increases very rapidly with M. DMRG avoids this problem by restricting the matrix dimension, using a variational relation, that maximizes the partition function. This idea is similar to what they do in the field of information theory, where they maximize entropy when they compress computational codes and image files.

Let us remind that the partition function is written as $Z = \mathrm{Tr}\,\rho_L = \omega_1^2 + \omega_2^2 + \cdots + \omega_r^2$. It has been known that ${\omega_i}^2$ decays rapidly when the correlation length of the system is finite, [20,40,41] and that the dumping rate is the decreasing function of the correlation length. Even at the critical temperature, we expect some decay in ${\omega_i}^2$, because the system size N is finite and the correlation length is at most N. As a result we can say that the partition function is well approximated as the sum of a few numbers of dominant eigenvalues

$$\bar{Z} \;=\; \sum_{i}^{m} {\omega_i}^2 \,, \tag{32}$$

where m is by far smaller than $r = \min(2^M, 2^{N-M})$. It is obvious that $Z \geq \bar{Z}$. We can also express Eq.22 as $\bar{Z} = \mathrm{Tr}\,(P_L\,\rho_L)$ using the projection operator

$$P_L(s'_{1\cdots}s'_M|s_{1\cdots}s_M) = \sum_{\xi_M=1}^{m} A(s'_{1\cdots}s'_M|\xi_M)A(s_{1\cdots}s_M|\xi_M)\,, \tag{33}$$

that satisfies $(P_L)^2 = P_L$ and $\mathrm{rank}\,P_L = m$; by the application of P_L, ξ_M is restricted to $1 \leq \xi_M \leq m$.

In the same way as we have restricted ξ_M (and ζ_{M+1}), we can restrict all the block spins in the matrix product

$$\bar{v}(s_{1\cdots}s_N) = \sum_{\{\xi\}\{\zeta\}}^{*m} \prod_{i=2}^{M} A(\xi_{i-1}s_i|\xi_i)\; \Omega(\xi_M|\zeta_{M+1}) \prod_{j=M+1}^{N-1} B(s_j\zeta_{j+1}|\zeta_j) \tag{34}$$

to obtain a variational state, where the symbol $*m$ denotes the freedom restrictions for ξ_2, ξ_3, $\cdots$ ξ_M, ζ_{M+1}, and ζ_{M+2}, $\cdots$ ζ_{N-1}; for example, when $m = 8$, the freedom of $s_1, \xi_2, \xi_3, \xi_4, \xi_5, \cdots$ $\zeta_{M-4}, \zeta_{M-3}, \zeta_{M-2}, \zeta_{M-1}, s_N$ are $2, 4, 8, 8, 8, \cdots 8, 8, 8, 4, 2$, respectively. If we take sufficiently large m, the largest eigenvalue of the transfer matrix can be well approximated as

$$\lambda_1 \geq \bar{\lambda}_1 \;=\; \frac{\bar{\boldsymbol{v}}^T\, T\, \bar{\boldsymbol{v}}}{\bar{\boldsymbol{v}}^T\, \bar{\boldsymbol{v}}} \;=\; \frac{\langle \bar{v}|T|\bar{v}\rangle}{\langle \bar{v}|\bar{v}\rangle}\,, \tag{35}$$

where the difference $\epsilon = \lambda_1 - \bar{\lambda}_1$ is a decreasing function of m. The denominator $\langle \bar{v}|\bar{v}\rangle$ is slightly smaller than 1.

6 Standard Form of the Variational State

Once we obtain the *exact* eigenvector $\boldsymbol{v}$ of the transfer matrix, we can exactly decompose it into the matrix product (Eqs.29), and can obtain a good variational state $\bar{\boldsymbol{v}}$ by restricting the dimension of matrices. (Eq.34) The mapping $\boldsymbol{v} \to \bar{\boldsymbol{v}}$ is, however, rather foolish because if we know $\boldsymbol{v}$ exactly, the eigenvalue problem for the transfer matrix T is already solved. What is necessary is to obtain a good variational state *without knowing* $\boldsymbol{v}$. The finite system algorithm provides us such a short cut.

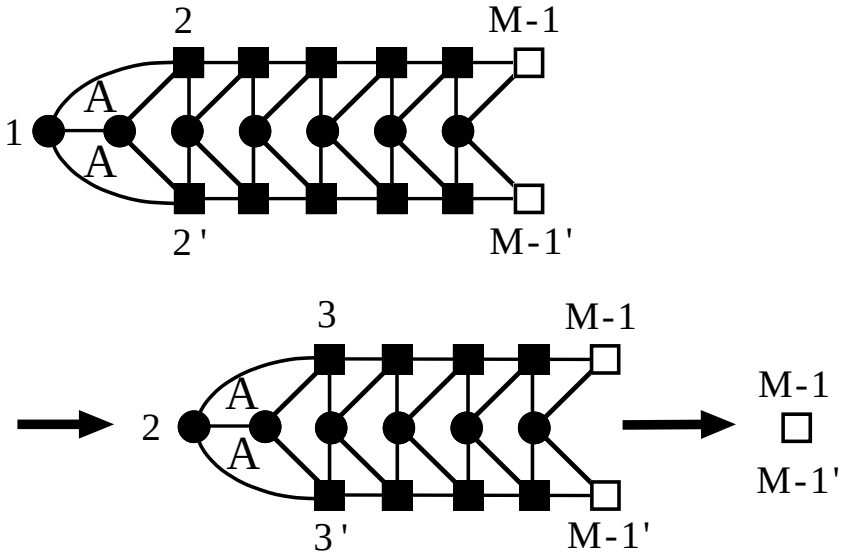

Fig. 4. Extended orthogonal relation for the matrix product in Eq.40.

The variational state $\tilde{v}(s_{1\cdots}s_N)$ used in DMRG is slightly different from the restricted matrix product that we have obtained in the last section. It has the form [42]

$$\sum_{\{\xi\}\{\zeta\}}^{*m} \prod_{i=2}^{M-1} \tilde{A}(\xi_{i-1}s_i|\xi_i)\, \tilde{V}(\xi_{M-1}s_M s_{M+1}\zeta_{M+2}) \prod_{j=M+2}^{N-1} \tilde{B}(s_j\zeta_{j+1}|\zeta_j)\,, \quad (36)$$

where the restricted sum is taken over for $\xi_2, \cdots \xi_{M-1}$ and $\zeta_{M+2}, \cdots \zeta_{N-1}$. The new state is different from $\bar{v}(s_{1\cdots}s_N)$ in Eq.34 in the following points: (1) The restricted matrices $\tilde{A}(\xi_{i-1}s_i|\xi_i)$ and $\tilde{B}(s_j\zeta_{j+1}|\zeta_j)$ satisfy the orthogonal relations

$$\sum_{\xi_{i-1}=1}^{*m} \sum_{s_i} \tilde{A}(\xi_{i-1}s_i|\xi_i)\, \tilde{A}(\xi_{i-1}s_i|\xi_i') \;=\; \delta_{\xi_i\,\xi_i'}$$

$$\sum_{s_j} \sum_{\zeta_{j+1}}^{*m} \tilde{B}(s_j\zeta_{j+1}|\zeta_j)\tilde{B}(s_j\zeta_{j+1}|\zeta'_j) \;=\; \delta_{\zeta_j\,\zeta'_j} \tag{37}$$

under the restriction where ξ_i *and* ζ_j *are at most* m.
(2) The new variational state contains $\tilde{V}(\xi_{M-1}s_M s_{M+1}\zeta_{M+2})$ that satisfies the normalization

$$\sum_{s_M s_{M+1}} \sum_{\xi_{M-1}\zeta_{M+2}}^{*m} \tilde{V}(\xi_{M-1}s_M s_{M+1}\zeta_{M+2})\,\tilde{V}(\xi_{M-1}s_M s_{M+1}\zeta_{M+2}) \;=\; 1\,. \tag{38}$$

(3) From (1) and (2), the new variational state is normalized $\langle\tilde{v}|\tilde{v}\rangle =$ (Eq.38) $= 1$, because the left and the right parts of the new variational state

$$\begin{aligned}
\tilde{A}(s_{1\cdots}s_{M-1}|\xi_{M-1}) \;&=\; \sum_{\xi_2\cdots\xi_{M-2}}^{*m} \prod_{i=2}^{M-1} \tilde{A}(\xi_{i-1}s_i|\xi_i) \\
\tilde{B}(s_{M+2\cdots}s_N|\zeta_{M+2}) \;&=\; \sum_{\zeta_{M+3}\cdots\zeta_{N-1}}^{*m} \prod_{j=M+2}^{N-1} \tilde{B}(s_j\zeta_{j+1}|\zeta_j)
\end{aligned} \tag{39}$$

satisfy the extended orthogonal relations (Fig.4)

$$\begin{aligned}
\sum_{s_1\cdots s_{M-1}} \tilde{A}(s_{1\cdots}s_{M-1}|\xi_{M-1})\tilde{A}(s_{1\cdots}s_{M-1}|\xi'_{M-1}) \;&=\; \delta_{\xi_{M-1}\xi'_{M-1}} \\
\sum_{s_{M+2}\cdots s_N} \tilde{B}(s_{M+2\cdots}s_N|\zeta_{M+2})\tilde{B}(s_{M+2\cdots}s_N|\zeta'_{M+2}) \;&=\; \delta_{\zeta_{M+2}\zeta'_{M+2}}
\end{aligned} \tag{40}$$

The normalization $\langle\tilde{v}|\tilde{v}\rangle = 1$ simplifies the variational relation $\lambda = \langle\tilde{v}|T|\tilde{v}\rangle/\langle\tilde{v}|\tilde{v}\rangle$ into the form

$$\tilde{\lambda}^{(M)} \;=\; \langle\tilde{v}|T|\tilde{v}\rangle \;=\; \sum_{\{s\}\{s'\}} \tilde{v}(s'_{1\cdots}s'_N)\,T(s'_{1\cdots}s'_N|s_{1\cdots}s_N)\,\tilde{v}(s_{1\cdots}s_N)\,, \tag{41}$$

where M is the position of $\tilde{V}$ in Eq.36.

We don't have to prepare 2^N-dimensional vector $\tilde{v}(s_{1\cdots}s_N)$ when we calculate $\tilde{\lambda}^{(M)}$. Figure 5 shows the graphical representation for $\tilde{\lambda}^{(M)}$. We first prepare $T_L(s'_1s'_2s'_3|s_1s_2s_3)$ and $T_R(s'_{N-2}s'_{N-1}s'_N|s_{N-2}s_{N-1}s_N)$, and perform the block-spin transformations

$$\begin{aligned}
&\tilde{T}_L(\xi'_2s'_3|\xi_2s_3) = \sum_{s'_1s'_2s_1s_2} \tilde{A}(s'_1s'_2|\xi'_2)T_L(s'_1s'_2s'_3|s_1s_2s_3)\tilde{A}(s_1s_2|\xi_2) \\
&\tilde{T}_R(s'_{N-2}\zeta'_{N-1}|s_{N-2}\zeta_{N-1}) = \\
&\sum_{s'_{N-1}s'_Ns_{N-1}s_N} \tilde{B}(s'_{N-1}s'_N|\zeta'_{N-1})T_R(s'_{N-2}s'_{N-1}s'_N|s_{N-2}s_{N-1}s_N)\tilde{B}(s_{N-1}s_N|\zeta_{N-1})
\end{aligned} \tag{42}$$

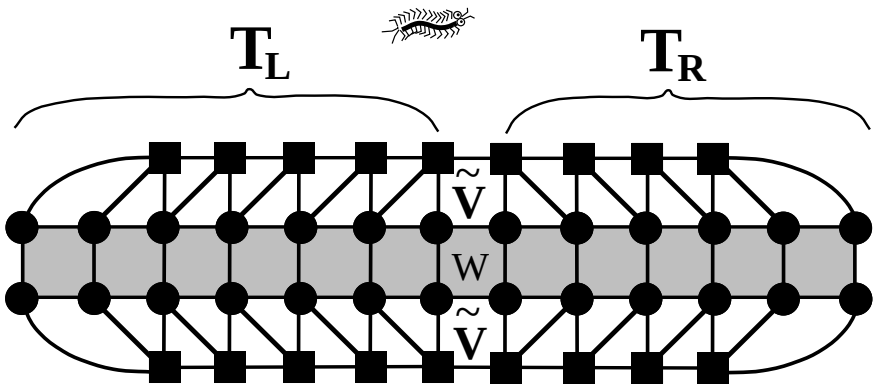

Fig. 5. Graphical representation for $\tilde{\lambda}^{(M)}$ in Eq.41. The shaded region is the transfer matrix in Eq.6.

to obtain $\tilde{T}_L$ and $\tilde{T}_R$. In general, when we have $\tilde{T}_L(\xi'_{i-1}s'_i|\xi_{i-1}s_i)$ and $\tilde{T}_R(s'_j\zeta'_{j+1}|s_j\zeta_{j+1})$ for a pair of i and j, we can obtain $\tilde{T}_L(\xi'_i s'_{i+1}|\xi_i\, s_{i+1})$ and $\tilde{T}_R(s'_{j-1}\zeta'_j|s_{j-1}\zeta_j)$ via the extension

$$\begin{aligned}\tilde{T}_L(\xi'_{i-1}s'_i s'_{i+1}|\xi_{i-1}s_i\, s_{i+1}) &= \tilde{T}_L(\xi'_{i-1}s'_i|\xi_{i-1}s_i)W(s'_i s'_{i+1}|s_i\, s_{i+1})\\ \tilde{T}_R(s'_{j-1}s'_j\zeta'_{j+1}|s_{j-1}s_j\zeta_{j+1}) &= W(s'_{j-1}s'_j|s_{j-1}s_j)\tilde{T}_R(s'_j\zeta'_{j+1}|s_j\zeta_{j+1})\end{aligned} \quad (43)$$

and the block-spin transformations

$$\begin{aligned}&\tilde{T}_L(\xi'_i s'_{i+1}|\xi_i\, s_{i+1})\\ &\quad=\sum_{s'_i s_i}\sum_{\xi'_{i-1}\xi_{i-1}}^{*m}\tilde{A}(\xi'_{i-1}s'_i|\xi'_i)\tilde{T}_L(\xi'_{i-1}s'_i s'_{i+1}|\xi_{i-1}s_i\, s_{i+1})\tilde{A}(\xi_{i-1}s_i|\xi_i)\\ &\tilde{T}_R(s'_{j-1}\zeta'_j|s_{j-1}\zeta_j)\\ &\quad=\sum_{s'_j s_j}\sum_{\zeta'_{j+1}\zeta_{j+1}}^{*m}\tilde{B}(s'_j\zeta'_{j+1}|\zeta'_j)\tilde{T}_R(s'_{j-1}s'_j\zeta'_{j+1}|s_{j-1}s_j\zeta_{j+1})\tilde{B}(s_j\zeta_{j+1}|\zeta_j)\,.\end{aligned} \quad (44)$$

After repeating Eq.43 and 44 for necessary times, we finally obtain $\tilde{T}_L(\xi'_{M-1}s'_M|\xi_{M-1}s_M)$ and $\tilde{T}_R(s'_{M+1}\zeta'_{M+2}|s_{M+1}\zeta_{M+2})$. We can construct the renormalized transfer matrix $\tilde{T}(\xi'_{M-1}s'_M s'_{M+1}\zeta'_{M+2}|\xi_{M-1}s_M s_{M+1}\zeta_{M+2})$ by

$$\tilde{T}_L(\xi'_{M-1}s'_M|\xi_{M-1}s_M)W(s'_M s'_{M+1}|s_M s_{M+1})\tilde{T}_R(s'_{M+1}\zeta'_{M+2}|s_{M+1}\zeta_{M+2})\,. \quad (45)$$

The variational eigenvalue $\tilde{\lambda}^{(M)}$ in Eq.41 is then expressed as

$$\begin{aligned}\tilde{\lambda}^{(M)} = \langle\tilde{V}|\tilde{T}|\tilde{V}\rangle = \sum_{\text{all indices}} &\tilde{V}(\xi'_{M-1}s'_M s'_{M+1}\zeta'_{M+2})\\ &\tilde{T}(\xi'_{M-1}s'_M s'_{M+1}\zeta'_{M+2}|\xi_{M-1}s_M s_{M+1}\zeta_{M+2})\tilde{V}(\xi_{M-1}s_M s_{M+1}\zeta_{M+2})\,.\end{aligned} \quad (46)$$

Thus we have calculated $\tilde{\lambda}^{(M)}$ without directly using the 2^N dimensional vector $\tilde{v}(s_{1\cdots}s_N)$.

7 Finite System Algorithm

The finite system algorithm improves the variational state $\tilde{v}(s_{1\cdots}s_N)$ (Eq.36) so that $\tilde{\lambda}^{(M)}$ is maximized. The algorithm gradually improves $\tilde{v}(s_{1\cdots}s_N)$, directly improving $\tilde{V}(\xi_{M-1}s_M s_{M+1}\zeta_{M+2})$, and indirectly improving other parts by shifting the place of $\tilde{V}$. The *local* improvement, which is maximization of $\tilde{\lambda}^{(M)}$, is performed through the diagonalization of the renormalized transfer matrix $\tilde{T}(\xi'_{M-1}s'_M s'_{M+1}\zeta'_{M+2}|\xi_{M-1}s_M s_{M+1}\zeta_{M+2})$. (We may call $\tilde{V}$ as the renormalized state vector.)

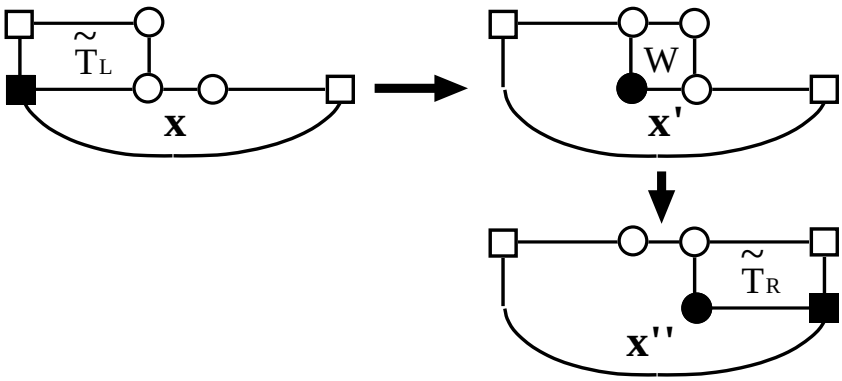

Fig. 6. Rapid multiplication of the renormalized transfer matrix to a vector. (Eq.47)

Numerical diagonalization for $\tilde{T}$ (Eq.45) is normally performed using the Lanczos method, [44] that requires multiplication of $\tilde{T}$ to a $4m^2$-dimensional vector $\boldsymbol{x}$. Since $\tilde{T}$ is represented as a product of $\tilde{T}_L$, W, and $\tilde{T}_R$, the numerical multiplication $\boldsymbol{x}''' = \tilde{T}\,\boldsymbol{x}$ can be done very rapidly along the way (Fig.6)

$$
\begin{aligned}
&x'(\xi'_{M-1}s'_M s_M s_{M+1}\zeta_{M+2}) \\
&\quad = \sum_{\xi_{M-1}}^{*m} \tilde{T}_L(\xi'_{M-1}s'_M|\xi_{M-1}s_M)x(\xi_{M-1}s_M s_{M+1}\zeta_{M+2})\,, \\
&x''(\xi'_{M-1}s'_M s'_{M+1}s_{M+1}\zeta_{M+2}) \\
&\quad = \sum_{s_M} W(s'_M s'_{M+1}|s_M s_{M+1})x'(\xi'_{M-1}s'_M s_M s_{M+1}\zeta_{M+2})\,,
\end{aligned}
$$

$$x'''(\xi'_{M-1}s'_M s'_{M+1}\zeta'_{M+2}) \tag{47}$$
$$= \sum_{s_{M+1}} \sum_{\zeta_{M+2}}^{*m} \tilde{T}_R(s'_{M+1}\zeta'_{M+2}|s_{M+1}\zeta_{M+2}) x''(\xi'_{M-1}s'_M s'_{M+1}s_{M+1}\zeta_{M+2}) ,$$

where we have to prepare $8m^2$-dimensional vector as the work space for computation. We don't have to create $4m^2$-dimensional transfer matrix $\tilde{T}$, that contains $16m^4$ numbers of matrix elements.

The finite system algorithm improves other parts of the variational state by shifting the place of $\tilde{V}$, where the procedure is to transform the variational state $\tilde{v}(s_{1\cdots}s_N)$ from the original form (Eq.36) to the new form

$$\sum_{\{\xi\}\{\zeta\}}^{*m} \prod_{i=2}^{M} \tilde{A}(\xi_{i-1}s_i|\xi_i)\, \tilde{V}(\xi_M s_{M+1}s_{M+2}\zeta_{M+3}) \prod_{j=M+3}^{N-1} \tilde{B}(s_j\zeta_{j+1}|\zeta_j) . \tag{48}$$

Compare the new expression to the old one (Eq.36), M is increased by one. This is similar to the relation between Eq.29 and Eq.30 in §4. The transformation is done by way of the following steps: [43,39]
(1) Create the normalized DSM $\tilde{\rho}_L(\xi'_{M-1}s'_M|\xi_{M-1}s_M)$ as

$$\sum_{s_{M+1}} \sum_{\zeta_{M+2}}^{*m} \tilde{V}(\xi'_{M-1}s'_M s_{M+1}\zeta_{M+2})\tilde{V}(\xi_{M-1}s_M s_{M+1}\zeta_{M+2}) . \tag{49}$$

(2) Then diagonalize the obtained DSM

$$\tilde{\rho}_L(\xi'_{M-1}s'_M|\xi_{M-1}s_M) = \sum_{\xi_M} \tilde{A}(\xi'_{M-1}s'_M|\xi_M)\, \tilde{\omega}_{\xi_M^2}\, \tilde{A}(\xi_{M-1}s_M|\xi_M) \tag{50}$$

to create the new orthogonal matrix $\tilde{A}(\xi_{M-1}s_M|\xi_M)$.
(3) Restrict the degree of freedom of ξ_M down to m.
(4) Create $\tilde{V}(\xi_M s_{M+1}s_{M+2}\zeta_{M+3})$ via the fusion of matrices (Fig.7)

$$\sum_{s'_M} \sum_{\xi'_{M-1}\zeta'_{M+2}}^{*m} \tilde{A}(\xi'_{M-1}s'_M|\xi_M)\tilde{V}(\xi'_{M-1}s'_M s_{M+1}\zeta'_{M+2})\tilde{B}(s_{M+2}\zeta_{M+3}|\zeta'_{M+2}) . \tag{51}$$

In such a way we can shift $\tilde{V}$ to the right direction. We can also shift $\tilde{V}$ to the left direction $M \to M-1$ by considering $\tilde{\rho}_R$.

Now the local improvement around M+1-th site is possible, via the maximization of $\tilde{\lambda}^{(M+1)}$. Since we have obtained $\tilde{A}(\xi_{M-1}s_M|\xi_M)$, we can easily obtain the shifted transfer matrix $\tilde{T}(\xi'_M s'_{M+1}s'_{M+2}\zeta'_{M+3}|\xi_M s_{M+1}s_{M+2}\zeta_{M+3})$ — increase M by one in Eq.45 — because we already have the matrix $\tilde{T}_R(s'_{M+2}\zeta'_{M+3}|s_{M+2}\zeta_{M+3})$ as a by-product of $\tilde{T}_R(s'_{M+1}\zeta'_{M+2}|s_{M+1}\zeta_{M+2})$, and we can obtain $\tilde{T}_L(\xi'_M s'_{M+1}|\xi_M s_{M+1})$ from $\tilde{T}_L(\xi'_{M-1}s'_M|\xi_{M-}s_M)$ just repeating the processes in Eqs.43 and 44 one more time for $\tilde{T}_L$.

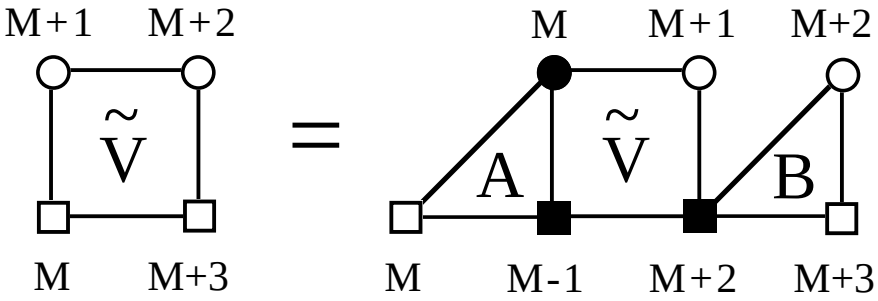

Fig. 7. Shift of the renormalized state vector $\tilde{V}$ by way of Eqs.49-51.

In such a way, we improve the variational state part by part, repeating the shift of $\tilde{V}$ and the local improvements around M. The finite system algorithm for classical systems is summarized as follows:

(1) Prepare the matrices $\tilde{A}$ and $\tilde{B}$, and a vector $\tilde{V}(\xi_{M-1}s_M s_{M+1}\zeta_{M+2})$ to express the initial variational state $\tilde{v}(s_{1\cdots}s_N)$ in Eq.36.
(2) Create $\tilde{T}_L(\xi'_{M-1}s'_M|\xi_{M-1}s_M)$ and $\tilde{T}_R(s'_{M+1}\zeta'_{M+2}|s_{M+1}\zeta_{M+2})$ using Eqs.43 and 44 for necessary times.
(3) Improve $\tilde{V}$ by the Lanczos diagonalization for the renromalized transfer matrix $\tilde{T} = \tilde{T}_L W \tilde{T}_R$; (Eqs.45.) maximize $\tilde{\lambda}^{(M)}$.
(4) Shift $\tilde{V}$ to the right direction, (Eqs.49-51) (Increment M by one.)
(5) Repeat (3) and (4) until $\tilde{V}$ reaches at the right end of the system.
(6) Shift $\tilde{V}$ to the left direction. (Decrement M by one.)
(7) Improve $\tilde{V}$ by Lanczos method, and repeat (6)-(7) until $\tilde{V}$ reaches at the left end of the system.
(8) Shuttle $\tilde{V}$ from the left to right by repeating the steps (3)-(7), and improve the all parts of the variational state.
(9) Stop the iteration when $\tilde{\lambda}^{(M)}$ converges to its maximum. [42]

It is interesting that they also use a similar shuttle process in the zero-temperature QMC simulation for fermionic system. [45]

In the above sequence, the Lanczos diagonalizations in step (3) and (7) always come after the shift of $\tilde{V}$ in (4) and (6). The shifted renormalized vector $\tilde{V}(\xi i-1\ s_i s_{i+1}\zeta_{i+2})$ (Eq.51) is a good candidates for the eigenvector of the shifted transfer matrix $\tilde{T}(\xi'_{i-1}s'_i s'_{i+1}\zeta'_{i+2}|\xi_{i-1}s_i s_{i+1}\zeta_{i+2})$. It is worth comparing Eq.29 (and Eq.30) and Eq.36 (and Eq.48) in order to understand why Eq.51 is efficient. We therefore choose them as the initial vector for the succeeding Lanczos diagonalizations, in order to accelerate the computation. [43,39]

After we complete all the processes (1)-(9), we obtain the maximized $\tilde{\lambda}^{(M)}$ and the corresponding variational state $\tilde{v}(s_{1\cdots}s_N)$. The variational free energy per site is expressed as

$$\tilde{f}^{(M)} = -\frac{1}{N}k_{\rm B}T\,\log\tilde{\lambda}^{(M)}\,, \tag{52}$$

and we can calculate thermodynamic quantities from the free energy. Since we have the variational state, we can directly calculate the spin correlation functions. For example, the spin polarization at the i-th site is obtained as

$$\langle s_i \rangle = \sum_{s_1 \cdots s_N} \tilde{v}(s_{1\cdots} s_i \cdots s_N)\, s_i\, \tilde{v}(s_{1\cdots} s_i \cdots s_N)\,, \tag{53}$$

and the diagonal two-spin correlation function is expressed in the same way

$$\langle s_i s_j \rangle = \sum_{s_1 \cdots s_N} \tilde{v}(s_{1\cdots} s_i \cdots s_j \cdots s_N)\, s_i\, s_j\, \tilde{v}(s_{1\cdots} s_i \cdots s_j \cdots s_N)\,. \tag{54}$$

We calculate $\langle s_i \rangle$ and $\langle s_i s_j \rangle$ without explicitly using $\tilde{v}(s_{1\cdots} s_N)$, as we have evaluated $\tilde{\lambda}^{(M)}$ without creating the 2^N-dimensional vector.

We have to pay attentions to the m-dependence of an observed thermodynamic quantity for N-site system, say $\theta(N,m)$, since there is an artificial energy scale ϵ_m that is introduced by the freedom restriction to the variational state. In order to get a reliable result for θ, ϵ_m should be smaller than the intrinsic energy scale of the system. When the system is off critical, ϵ_m should be smaller than the energy gap of the system ϵ_g, which is of the order of ${\ell_0}^{-1}$, where ℓ_0 is the correlation length of the system. When the system is in the critical region, the energy scale $\epsilon_N \sim O(1/N)$ introduced by the system size is larger than $\epsilon_g \sim 0$, and therefore ϵ_m should be smaller than ϵ_N. In both cases, we have to calculate $\theta(N,m)$ for several different m, and estimate the infinite m limit $\theta(N,\infty)$; this is not difficult, because $\theta(N,m)$ loses the m-dependence when m is sufficiently large. At criticality we have to further perform the finite size scaling (FSS) analyses [46,47] for $\theta(N,\infty)$ with respect to N to obtain $\theta(\infty,\infty)$ [48], and other observables such as critical indices [6–8] or the latent heat. [49]

One might not happy about the construction of initial variational state in the initial step (1). Roughly speaking, we may choose arbitrary $\tilde{A}$, $\tilde{B}$, and $\tilde{V}(\xi_{M-1} s_M s_{M+1} \zeta_{M+2})$. The initial matrices do not have to satisfy the orthogonal relations Eq.39, because they are automatically orthogonalized during the first sweep of $\tilde{V}$. If the system is uniform, [50] i.e. the local Boltzmann weights $W(s'_{i-1} s'_i | s_{i-1} s_i)$ do not depend on their position, we can create the initial variational state by the infinite system algorithm.

8 Infinite System Algorithm

Suppose that the system is off critical, and the system size N is far larger than the correlation length ℓ_0. Under this situation the variational state $\tilde{v}(s_{1\cdots} s_N)$ obtained by the finite system algorithm (Eq.36) has the following properties:

(1) The matrices $\tilde{A}(\xi_{i-1} s_i | \xi_i)$ and $\tilde{B}(s_j \zeta_{j+1} | \zeta_j)$ are almost position independent deep inside the system $i \gg \ell_0$ and $N - j \gg \ell_0$. [30]

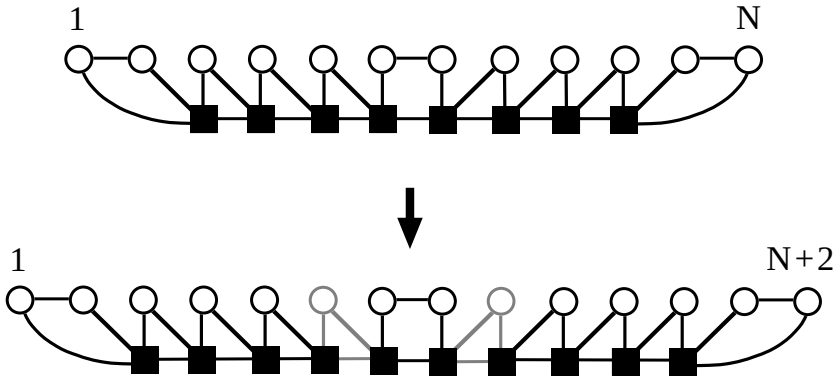

Fig. 8. Similarity between N-site system and $N+2$-site system: we can get the variational state for the latter by just inserting two matrices to the former.

(2) The matrices near the both end of the system are functions of the distance from the boundary, i.e., i and $N-j$, and they are not dependent on N.

The variational state is therefore uniform except for the 'skins' near the boundary. From the fact we can say that the variational state $\tilde{v}(s_{1\cdots}s_N)$ is almost identical to the corresponding parts of variational state $\tilde{v}(s_{1\cdots}s_{N+2})$ for the $N+2$-site system. (Fig.8) The correspondence between $\tilde{v}(s_{1\cdots}s_N)$ and $\tilde{v}(s_{1\cdots}s_{N+2})$ shows that if we already have the former, we can create the latter by just inserting two matrices at the center. If we are interested in the bulk property of the system, what we need is the position independent matrices inside the system, and we don't have to obtain the variational state $\tilde{v}(s_{1\cdots}s_N)$ near the boundary so accurately. The infinite system algorithm creates such a uniform part of the variational state through the correspondence between N and $N+2$.

The algorithm starts from the 4-site system, whose transfer matrix is

$$T(s_1's_2's_{\overline{2}}'s_{\overline{1}}'|s_1s_2s_{\overline{2}}s_{\overline{1}}) = T_L(s_1's_2'|s_1s_2)W(s_2's_{\overline{2}}'|s_2s_{\overline{2}})T_R(s_{\overline{2}}'s_{\overline{1}}'|s_{\overline{2}}s_{\overline{1}})\,. \quad (55)$$

We have used the site indices $1, 2, \overline{2}, \overline{1}$ instead of $1, 2, 3, 4$, in order to stress that the right half of the system has the same size as the left half. Diagonalizing the transfer matrix, we obtain the largest eigenvalue and the corresponding eigenvector $v(s_1s_2s_{\overline{2}}s_{\overline{1}})$. Then we decompose it

$$v(s_1s_2s_{\overline{2}}s_{\overline{1}}) \;=\; \sum_{\xi_2} A(s_1s_2|\xi_2)\,\omega_{\xi_2}\,B(s_{\overline{2}}s_{\overline{1}}|\xi_2) \quad (56)$$

using SVD. The trick in the infinite system algorithm is to use the matrices $\tilde{A}(s_1s_2|\xi_2)$ and $\tilde{B}(s_{\overline{2}}s_{\overline{1}}|\zeta_{\overline{2}})$ as block spin transformations for the 6-site system.

The procedure is to increase the system size

$$\begin{aligned} T_L(s_1' s_2' s_3' | s_1 s_2 s_3) &= T_L(s_1' s_2' | s_1 s_2) W(s_2' s_3' | s_2 s_3) \\ T_R(s_{\overline{3}}' s_{\overline{2}}' s_{\overline{1}}' | s_{\overline{3}} s_{\overline{2}} s_{\overline{1}}) &= W(s_{\overline{3}}' s_{\overline{2}}' | s_{\overline{3}} s_{\overline{2}}) T_R(s_{\overline{2}}' s_{\overline{1}}' | s_{\overline{2}} s_{\overline{1}}) , \end{aligned} \tag{57}$$

and then to apply the block spin transformation

$$\begin{aligned} \tilde{T}_L(\xi_2' s_3' | \xi_2 s_3) &= \sum_{s_1' s_1 s_2' s_2} \tilde{A}(s_2' s_1' | \xi_2') \tilde{T}_L(s_1' s_2' s_3' | s_1 s_2 s_3) \tilde{A}(s_2 s_1 | \xi_2) \\ \tilde{T}_R(s_{\overline{3}}' \zeta_{\overline{2}}' | s_{\overline{3}} \zeta_{\overline{2}}) &= \sum_{s_{\overline{2}}' s_{\overline{2}} s_{\overline{1}}' s_{\overline{1}}} \tilde{B}(s_{\overline{2}}' s_{\overline{1}}' | \zeta_{\overline{2}}') \tilde{T}_R(s_{\overline{3}}' s_{\overline{2}}' s_{\overline{1}}' | s_{\overline{3}} s_{\overline{2}} s_{\overline{1}}) \tilde{B}(s_{\overline{2}} s_{\overline{1}} | \zeta_{\overline{2}}) \end{aligned} \tag{58}$$

to obtained the renormalized transfer matrix for $N = 6$

$$\tilde{T}(\xi_2' s_3' s_{\overline{3}}' \zeta_{\overline{2}}' | \xi_2 s_3 s_{\overline{3}} \zeta_{\overline{2}}) = \tilde{T}_L(\xi_2' s_3' | \xi_2 s_3) W(s_3' s_{\overline{3}}' | s_3 s_{\overline{3}}) \tilde{T}_R(s_{\overline{3}}' \zeta_{\overline{2}}' | s_{\overline{3}} \zeta_{\overline{2}}) , \tag{59}$$

whose eigenvector is $\tilde{V}(\xi_2 s_3 s_{\overline{3}} \zeta_{\overline{2}})$. Equations 58 and 59 are similar to Eqs.43 and 44, respectively. Since we have applied the matrices $\tilde{A}$ and $\tilde{B}$, that are obtained from 4-site system to the transfer matrix for $N = 6$, the block spin transformation (Eq.58) is different from the best one. We don't mind this point, because the aim of the infinite system algorithm is to obtain the uniform matrix product state in the thermodynamic limit $N \to \infty$. [30] We just repeat the extension of the transfer matrix (Eq.57) and the block spin transformation (Eq.58) to arbitrary system size along the sequence

$$\begin{aligned} T(s_1' s_2' s_{\overline{2}}' s_{\overline{1}}' | s_1 s_2 s_{\overline{2}} s_{\overline{1}}) &\to \tilde{T}(\xi_2' s_3' s_{\overline{3}}' \zeta_{\overline{2}}' | \xi_2 s_3 s_{\overline{3}} \zeta_{\overline{2}}) \to \cdots \\ &\cdots \to \tilde{T}(\xi_i' s_{i+1}' s_{\overline{i+1}}' \zeta_{\overline{i}}' | \xi_i \, s_{i+1} s_{\overline{i+1}} \zeta_{\overline{i}}) \to \ldots , \end{aligned} \tag{60}$$

until finally the eigenvector $\tilde{V}(\xi_i s_{i+1} s_{\overline{i+1}} \zeta_{\overline{i}})$ converges to its fixed point. Equations 55-60 are the outline of the infinite system algorithm for classical systems.

The lanczos diagonalization for the renormalized transfer matrix can be performed very rapidly if we choose the eigenvectors in the previous Lancozs diagonalization as the starting vector for the next diagonalization. (There are better constructions of the initial vector. [39,43])

There are two usages of the infinite system algorithm. One is to use it as a preparation for the finite system algorithm. After repeating the above iteration (Eqs.57-58) for $N/2$ times, we obtain all the matrices and vectors, that are necessary to start the finite system DMRG algorithm for the N-site system. [1]

The other usage of the infinite system algorithm is to use it purely in order to obtain the thermodynamic limit of the variational state. We reach the fixed point when the iteration time i is several times larger than the

correlation length ℓ_0. [30,52] Using the fixed point matrices, we can calculate the thermal average of operators, such as the spin polarization

$$\langle s_i \rangle = \sum_{\xi_{i-1} s_i s_{\bar{i}} \zeta_{\overline{i-1}}} \tilde{V}(\xi_{i-1} s_i s_{\bar{i}} \zeta_{\overline{i-1}})\, s_i\, \tilde{V}(\xi_{i-1} s_i s_{\bar{i}} \zeta_{\overline{i-1}})\,, \tag{61}$$

and the nearest neighbor spin correlation function

$$\langle s_i s_{\bar{i}} \rangle = \sum_{\xi_{i-1} s_i s_{\bar{i}} \zeta_{\overline{i-1}}} \tilde{V}(\xi_{i-1} s_i s_{\bar{i}} \zeta_{\overline{i-1}})\, s_i s_{\bar{i}}\, \tilde{V}(\xi_{i-1} s_i s_{\bar{i}} \zeta_{\overline{i-1}})\,, \tag{62}$$

where both $\langle s_i \rangle$ and $\langle s_i s_{\bar{i}} \rangle$ are independent to the index i. It is also possible to calculate spin correlation functions between distant sites, as we have done in finite system algorithm. (See Eq.54)

For the calculation of spin correlation functions, we have to check that the energy scale ϵ_m introduced by the freedom restriction is smaller than the intrinsic energy scale ϵ_g of the system; we have to use sufficiently large m where the calculated results are not dependent on m.

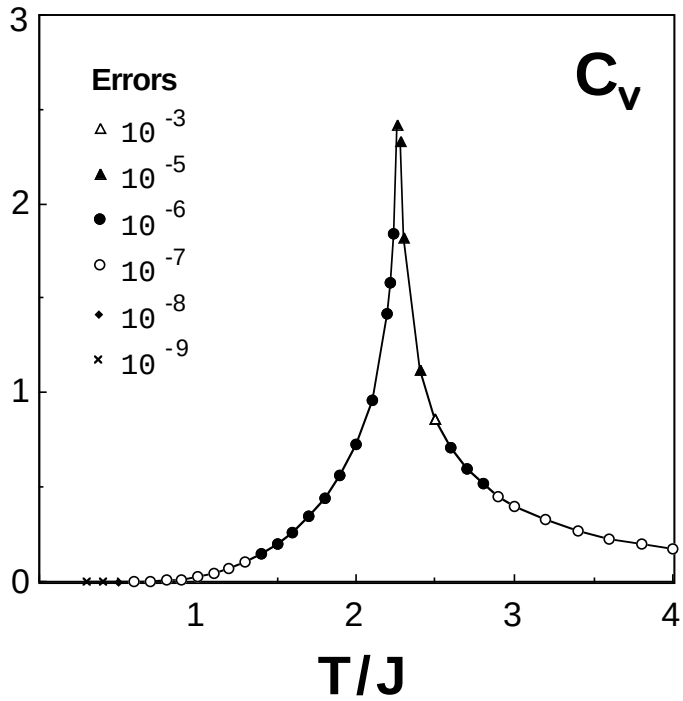

Fig. 9. Calculated specific heat of the Ising model. [5]

Let us see how precise the infinite DMRG is. Figure 9 shows the specific heat $C_v(T)$ of the square lattice Ising model, which is obtained by taking the temperature derivative of the nearest neighbor correlation function $E(T) = \langle s_i s_{\bar{i}} \rangle$. We calculate $E(T)$ for the system with $N = 2i = 2048$, which is sufficiently larger than the correlation length for each plotted temperature. The m dependence for $E(T)$ is not conspicuous for $m = 60$. Since we know the exact solution for this model, we can directly evaluate the numerical error in $C_v(T)$. The difference between calculated $C_v(T)$ and the exact one is indicated by several different marks. The numerical error is non-negligible near the critical temperature T_c, partly because $E(T)$ is singular at T_c, and because numerical derivative

$$\frac{E(T + \Delta T/2) - E(T - \Delta T/2)}{\Delta T} \tag{63}$$

is sensitive to ΔT; typically, we choose $\Delta T = 10^{-4}$. The other source of numerical error is that the increase of cut-off energy scale ϵ_m near T_c, that spoils the numerical precision in block spin transformation. The latter error source can be suppressed by scaling analysis for m. [**?**]

9 Discussion

We have considered the 2D Ising model on a cylinder, and applied DMRG using a variational relation (Eq.1) for the partition function. (Fig.1) The block spin transformation is obtained from the diagonalization of DSM, which corresponds to a cut on the cylinder. The pictorial image of the DSM (Fig.1) suggests that we can define DSM for a 2D classical system with arbitrary shape, for the purpose of applying DMRG to it. It is surprising that Baxter established such a construction of DSM more than 30 years ago. [19,20] He considered a square cluster, and expressed the partition function of the stem as a 4-th power of the corner transfer matrix. (CTM) He then use a variational relation, which is essentially the same as that in DMRG, [53] to maximize the partition function. He calculated the variational free energy using a self-consistent equation, that is quite similar to the infinite system algorithm in DMRG. The advantage of Baxter's method is that the numerical calculation is very fast, because it does not require the Lanczos diagonalization of the row-to-row transfer matrix. Nishino and Okunishi introduced this advantage to DMRG, and formulated the 'corner transfer matrix renormalization group.' [54,48] (CTMRG)

Figure 10 (a) shows the construction of DSM in CTMRG. In CTMRG and Baxter's method, the DSM correspond to a cut on a square cluster. Such a construction of DSM can be generalized to any dimension. [55] For example, in 3D, the DSM for a cubic system corresponds to a cut on the cube, shown as Fig.10 (b). As we have expressed the DSM for 2D square as a 4-th power of CTM, the DSM for 3D cube is expressed as a contraction between 8 *corner*

general principle for such a discretization, that is suitable for DMRG.
We hope that these problems will be solved near future.

The authors thank to all the organizers of DMRG '98 workshop at Max-Planck-Institute für Physik komplexer System in Dresden. T. N thank to I. Peschel, E. Carlon, G. Sierra and M. A. Martìn-Delgado about the discussions for classical systems. Numerical calculations were done using NEC SX-4 in the computer center of Osaka University. Y. H. is partly supported by the Sasakawa Scientific Research Grant from The Japan Science Society. K. O. and T. H. partially supported by a Grant-in-Aid from the Ministry of Education, Science and Culture of Japan.

References

1. S. R. White: Phys. Rev. Lett. **69** (1992) 2863; Phys. Rev. **B 48** (1993) 10345; see also his review in this textbook.
2. H. F. Trotter: Proc. Am. Math. Soc. **10** (1959) 545.
3. M. Suzuki: Prog. Theor. Phys. **56** (1976) 1454.
4. R. P. Feynmann and A. R. Hibbs: *Quantum Mechanics and Path Integrals* (McGraw-Hill, 1965).
5. T. Nishino, J. Phys. Soc. Jpn. 64, No.10 (1995) 3598.
6. Enrico Carlon and Andrzej Drzewiński: Phys. Rev. Lett. **79** (1997) 1591; Phys. Rev. **E57** (1998) 2626; also see their articles in this book.
7. Enrico Carlon and Ferenc Igloi: Phys. Rev. B 57, 7877 (1998); Ferenc Igloi and Enrico Carlon: cond-mat/9805083.
8. Enrico Carlon, Andrzej Drzewiński and Jos Rogiers: cond-mat/cond-mat/9803193.
9. R. J. Bursill, T. Xiang, G. A. Gehring: J. Phys. Condensed Matter (1996) L583-L590.
10. X. Wang and T. Xiang, Phys. Rev. **B56** 5061 (1997); also see their articles in this book.
11. N. Shibata, J. Phys. Soc. Jpn **66**, 2221 (1997); also see his article in this book.
12. H. A. Kramers and G. H. Wannier: Phys. Rev. **60** (1941) 263.
13. R. Kikuchi: Phys. Rev. **81** (1951) 988.
14. To treat an asymmetric transfer matrix is not rare in statistical mechanics; see Baxter's Textbook. [20] Also, please read ref.10 and 11.
15. H. A. Bethe: Proc. Roy. Soc. **A150** (1935) 552.
16. M. C. Gutzwiller: Phys. Rev. **137** (1965) A1726.
17. J. Kanamori: J. Phys. Soc. Jpn. **30** (1963) 275.
18. J. Hubbard: Proc. Roy. Soc. **A276** (1963) 238; **A281** (1964) 401.
19. R. J. Baxter: J. Math. Phys. **9** (1968) 650; R. J. Baxter: J. Stat. Phys. **19** (1978) 461.
20. R. J. Baxter: *Exactly Solved Models in Statistical Mechanics* (Academic Press, London, 1982).
21. N. P. Nightingale and H. W. Blöte: Phys. Rev. **B33** (1986), 659.
22. I. Affleck, T. Kennedy, E. H. Lieb and H. Tasaki: Phys. Rev. Lett. **59** (1987) 799.

23. M. Fannes, B. Nachtergale and R. F. Werner: Europhys. Lett. **10** (1989) 633; M. Fannes, B. Nachtergale and R. F. Werner: Commun. Math. Phys. **144** (1992) 443; M. Fannes, B. Nachtergale and R. F. Werner: Commun. Math. Phys. **174** (1995) 477.
24. A. Klümper, A. Schadschneider and J. Zittarz: Z. Phys. **B87** (1992) 281; H. Niggemann, A. Klümper and J. Zittartz: Z. Phys. **B104** (1997) 103.
25. B. Derrida and M. R. Evans : J.Phys.A: Math. Gen. **26** (1993) 1493.
26. N. Rajewsky, L. Santen, A. Schadschneider, M. Schreckenberg; cond-mat/9710316.
27. A. Honecker, I. Peschel: J. Stat. Phys. **88** (1997)319.
28. Y. Hieida; preprint.
29. A modification of the whole part of the variational state is more time consuming. The situation is similar to the 'Order N' problem in the density functional formalism.
30. S. Östlund and S. Rommer: Phys. Rev. Lett **75** (1995) 3537; S. Rommer and S. Östlund: Phys. Rev. **B55** (1997) 2164; M. Andersson, M. Boman, and S. Östlund: cond-mat/9810093.
31. M. A. Martin-Delgado, G. Sierra: Int. J. Mod. Phys. **A11** (1996) 3145.
32. G. Sierra and M. A. Martín-Delgado: *Strongly Correlated Magnetic and Superconducting Systems,* (Springer Berlin, 1997), and references there in.
33. It is possible to fix the boundary spins to consider more general boundary conditions.
34. F. Y. Wu: Rev. Mod. Phys. **54** (1982) 235, and references there in.
35. There is a bibliography of Ising in cond-mat/9605174.
36. Baxter used another definition of the density submatrix in his variational method, ref.20 where his density submatrix is block diagonal. It is possible to reformulate DMRG using Baxter's density submatrix.
37. Density submatrices have negative eigenvalues when the system contains randomness.
38. The *Numerical recipes Home Page* (http://cfata2.harvard.edu/numerical-recipes/) is useful to know about numerical linear algebra. Also it is worth reading J. Wilkinson: *The Algebraic Eigenvalue Problem* (Oxford, London, 1965).
39. T. Nishino and K. Okunishi: J. Phys. Soc. Jpn. **64** (1995) 4084.
40. I. Peschel, M. Kaulke, and Ö. Legeza: cond-mat/9810174; also see their article in this book.
41. K. Okunishi, Y. Hieida, and Y. Akutsu: cond-mat/9810239.
42. H. Takasaki, T. Hikihara, and T. Nishino: cond-mat/9810241.
43. S. R. White: Phys. Rev. Lett. **77** (1996) 3633.
44. C. Lanczos: J. Res. Nat. Bur. Std. **45** (1950) 255.
45. S. R. White, D. J. Scalapino, R. L. Sugar, E. Y. Loh, J. E. Gubernatis and R. T. Scalettar: Phys. Rev. **B40** (1989) 506.
46. M. E. Fisher: in *Proc. Int. School of Physics 'Enrico Fermi'*, edited by M.S. Green, (Academic Press, New York, 1971), Vol. **51**, p. 1.
47. M. N. Barber: in *Phase Transitions and Critical Phenomena*, edited by C. Domb and J. L. Lebowitz, (Academic Press, New York, 1983), Vol. **8**, p. 146. and references therein.
48. T. Nishino, K. Okunishi, and M. Kikuchi: Physics Letters **A213** (1996) 69.
49. T. Nishino and K. Okunishi: J. Phys. Soc. Jpn. **67** (1998) 1492.
50. Position dependence *in quantum Hamiltonian* can be treated by infinite system DMRG; K. Hida: J. Phys. Soc. Jpn. **65** (1996) 895.

51. U. Schollvöck, cond-mat/9804231.
52. It is not a good idea to use the infinite system algorithm just at the critical temperature, because ℓ_0 is infinite.
53. K. Okunishi: Thesis, Osaka University 1997 (in Japanese); Thesis (in preparation).
54. T. Nishino and K. Okunishi: J. Phys. Soc. Jpn. **65** (1996) 891; T. Nishino and K. Okunishi: J. Phys. Soc. Jpn. **66** (1997) 3040.
55. T. Nishino and K. Okunishi: J. Phys. Soc. Jpn. **67** (1998) 3066.
56. Numerical precision in DMRG for a system with periodic boundary condition is lower than that for the system with open boundary condition. The reason can be understood by looking at the variational state written in matrix product.